

Pressure dependence of the exchange interaction in the dimeric single-molecule magnet $[\text{Mn}_4\text{O}_3\text{Cl}_4(\text{O}_2\text{CET})_3(\text{py})_3]_2$ from inelastic neutron scattering

A. Sieber,¹ D. Foguet-Albiol,² O. Waldmann,¹ S. T. Ochsenbein,¹ G. Carver,¹ H. Mutka,³ F. Fernandez-Alonso,⁴ M. Mezouar,⁵ H. P. Weber,^{6,7} G. Christou,² and H. U. Güdel¹

¹Department of Chemistry and Biochemistry, University of Bern, 3012 Bern, Switzerland

²Department of Chemistry, University of Florida, Gainesville, Florida 32611, USA

³Institut Laue-Langevin, 6 Rue Jules Horowitz, Boîte Postale 156, 38042 Grenoble Cedex 9, France

⁴ISIS Facility, CCLRC Rutherford Appleton Laboratory, Chilton, Didcot, Oxfordshire OX11 0QX, United Kingdom

⁵European Synchrotron Radiation Facility, 6 Rue Jules Horowitz, Boîte Postale 220, 38043 Grenoble Cedex 9, France

⁶ACCE, 38960 St Aupre, France

⁷Laboratoire de Crystallographie EFPL-FSB-IPMC, BSP-Dorigny, 1015 Lausanne, Switzerland

(Received 29 March 2006; published 10 July 2006)

The low-lying magnetic excitations in the dimers of single-molecule magnets $[\text{Mn}_4\text{O}_3\text{Cl}_4(\text{O}_2\text{CET})_3(\text{py})_3]_2$, or $(\text{Mn}_4)_2$, are studied by inelastic neutron scattering as a function of hydrostatic pressure. The anisotropy parameters D and B_0^4 , which describe each Mn_4 subunit, are essentially pressure independent, while the antiferromagnetic exchange coupling J between the two Mn_4 subunits strongly depends on pressure, with an increase of 42% at 17 kbar. Additional pressure-dependent powder x-ray measurements allow a structural interpretation of the findings.

DOI: 10.1103/PhysRevB.74.024405

PACS number(s): 75.50.Xx, 61.12.Ex, 75.10.Jm, 81.40.Vw

Molecular magnetic clusters have attracted considerable attention recently because of the striking quantum phenomena observed in these systems.^{1–6} The so-called single-molecule magnets (SMMs), for instance, exhibit magnetization hysteresis and quantum tunneling of magnetization (QTM) at low temperatures.^{7–9}

An important issue in this context is the weak magnetic interactions between individual clusters (*intermolecular* interactions), as mediated by weak long-distance superexchange paths like hydrogen bonds. On the one hand, this kind of interaction has to be considered seriously in potential applications as they would tend to degrade the performance. On the other hand, new physical phenomena can emerge, e.g., field-induced long-range ordering in weakly interacting antiferromagnetic (AFM) clusters.¹⁰ Such phenomena are currently of great interest with regard to magnetization plateaus in quantum spin systems or Bose-Einstein condensation of magnons.^{11,12} Furthermore, intermolecular magnetic interactions between SMMs can provide highly desirable situations, as in the exchange-biased SMM $[\text{Mn}_4\text{O}_3\text{Cl}_4(\text{O}_2\text{CET})_3(\text{py})_3]_2$, or $(\text{Mn}_4)_2$ (EtCO_2^- is propionate, py is pyridine). Its dimer structure, shown in Fig. 1, consists of two Mn_4 monomers which are weakly coupled to each other by AFM exchange interactions mediated by $\text{C-H}\cdots\text{Cl}$ hydrogen bonds and close $\text{Cl}\cdots\text{Cl}$ contact (see Fig. 1). The effect of the weak AFM coupling is striking; it results in a magnetic hysteresis curve with QTM completely suppressed at zero field,¹³ in contrast to the behavior of generic SMMs. A precise understanding of intermolecular interactions between molecular magnetic clusters, SMMs in particular, is thus important from both the applications and fundamental points of view.

In this work, the pressure dependence of the AFM interaction, of strength J , between the Mn_4 subunits in $(\text{Mn}_4)_2$ is studied by inelastic neutron scattering (INS). The results were complemented with pressure-dependent powder x-ray measurements. These are the first pressure experiments of a

molecular magnetic compound with weak intermolecular interactions to our knowledge. As a main result a pronounced pressure dependence of J is found, which correlates with the weak bonds between the Mn_4 subunits in $(\text{Mn}_4)_2$. Our results further suggest a strong effect of pressure on the magnetic hysteresis curve of $(\text{Mn}_4)_2$.

Partially deuterated microcrystalline samples of $(\text{Mn}_4)_2$, $[\text{Mn}_4\text{O}_3\text{Cl}_4(\text{O}_2\text{CET})_3(\text{py-d}_5)_3]_2\cdot 8\text{CH}_3\text{CN}$, were freshly prepared following Ref. 14, and checked by x-ray powder diffraction and elemental analysis. The INS experiments were performed on IN5 at the Institut Laue-Langevin (ILL) in Grenoble, France, and on IRIS at the ISIS Facility, CCLRC

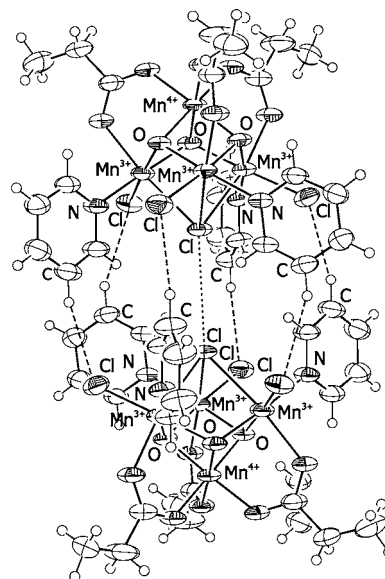


FIG. 1. Structure of $(\text{Mn}_4)_2$. The molecule exhibits a threefold symmetry axis which passes through the two Mn^{4+} ions. The dashed lines indicate the six $\text{C-H}\cdots\text{Cl}$ hydrogen bonds, and the dotted line the close $\text{Cl}\cdots\text{Cl}$ approach.

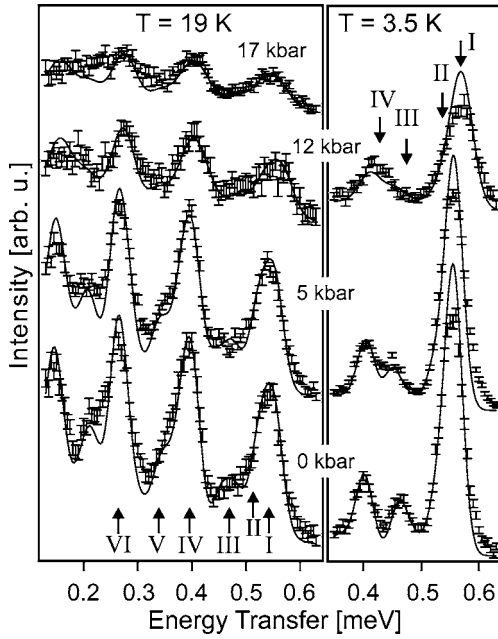


FIG. 2. INS spectra of $(\text{Mn}_4)_2$ recorded on IN5 (data for 0, 5, and 12 kbar at 19 and 3.5 K) and IRIS (data for 17 kbar at 19 K). Data were background corrected. The labeling of the peaks corresponds to Fig. 3 (and Ref. 17). The solid lines represent the simulated spectra with the best-fit parameters, and an instrumental resolution of $35 \mu\text{eV}$ for 0 and 5 kbar and $45 \mu\text{eV}$ for 12 and 17 kbar (the lower resolution at 12 and 17 kbar is attributed to the larger pressure inhomogeneities in clamp cells as compared to He cells).

Rutherford Appleton Laboratory in Chilton, U.K. Spectra were acquired in the temperature range 1.5–20 K. On IN5, data were collected for several pressures up to 12 kbar with an incident wavelength $\lambda_i = 7.0 \text{ \AA}$. The instrumental resolution was $31 \mu\text{eV}$ at the elastic line. On IRIS, data were recorded at 17 kbar using a pyrolytic graphite (PG002) analyzer with a final wavelength $\lambda_f = 6.6 \text{ \AA}$. The resolution was $17.5 \mu\text{eV}$ at the elastic line. In both experiments the data were corrected for detector efficiency using a vanadium standard. The spectra correspond to the sum over all detectors. Further data treatment included subtraction of the background by approximating it with a suitable analytical function (this function was obtained from the 1.5 K spectrum, which exhibits the lowest number of magnetic peaks). For the pressures $p=0$ and 5.0(1) kbar, a standard ILL continuously loaded high-pressure He gas cell was used (3.7 g sample). For $p=12.0(5)$ kbar the standard ILL 15 kbar high-pressure clamp cell (0.4 g sample), and for $p=17.0(5)$ kbar a McWhan high-pressure clamp cell (0.5 g sample) was used, in both cases with FC-75 (fluorinated hydrocarbon, 3M) as pressure-transmitting medium. In all experiments cooling was achieved with an Orange cryostat.

High-resolution powder diffraction data were collected at ambient temperature and pressures up to 40 kbar on beamline ID27 at the ESRF, Grenoble. A finely ground powder sample was inserted into a diamond-anvil cell, with FC-75 as pressure-transmitting medium, an Inconel gasket to contain the sample, and a ruby crystal as pressure calibrant. A wavelength of 0.3738 \AA was selected with a Si double-crystal

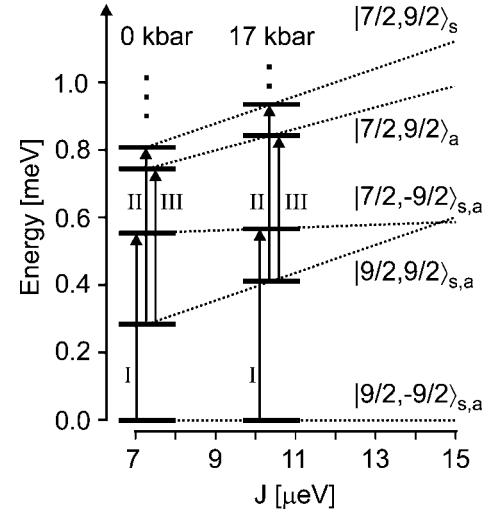


FIG. 3. Energy level diagram of $(\text{Mn}_4)_2$ as function of J ($D = -62.4 \mu\text{eV}$, $B_4^0 = -7.2 \times 10^{-3} \mu\text{eV}$). The arrows assign the transitions seen in Fig. 2 at 0 and 17 kbar. The notation for the approximate wave functions is $|M_{S_A}, M_{S_B}\rangle_{s/a} = (|M_{S_A}, M_{S_B}\rangle \pm |M_{S_B}, M_{S_A}\rangle) / \sqrt{2}$ (see Ref. 17).

monochromator. The beam was focused to $5 \mu\text{m}$ at the sample. The diffracted x rays were detected with a MAR345 image plate. Exposure times were of the order of minutes in single-bunch mode. The two-dimensional diffraction data were projected to 1D using the program FIT2D.¹⁵ The peak positions were determined with the program FULLPROF using the profile-fitting mode. The space group was determined to $R\bar{3}$. The unit-cell parameters a and c were obtained from least-squares fitting the positions of the first ten clearly resolved peaks in the angular range $1.6^\circ < 2\theta < 4.0^\circ$.

Figure 2 presents the neutron energy-loss side of the INS spectra recorded at 19 and 3.5 K for pressures from 0 to 17 kbar. Several peaks were observed at transfer energies below 0.6 meV. The 0 kbar data are fully consistent with our previous ambient pressure INS experiment,¹⁷ and the peaks were labeled the same way. The broad asymmetric peak at ca. 0.55 meV in fact consists of two close transitions, peak I, which is the only cold transition, and peak II, which at 3.5 K already has significant intensity. At 3.5 K peaks III and IV also have significant intensities, and at higher temperatures many more transitions show up at lower energy transfers. The assignment of the transition I-III is shown in Fig. 3; for a complete discussion of the 0 kbar spectra and assignment of the peaks we refer to Ref. 17. With increasing pressure, the spectra show significant changes, most notably shifts in the positions of peaks I and III. Peak I clearly moves to higher energies with increasing pressure (the position of peak II is largely unaffected), while peak III moves to lower energy and approaches peak IV, overlapping with it at the highest pressures.

As demonstrated from magnetization,¹³ electron spin resonance,⁴ and INS measurements,¹⁷ the low-temperature magnetism in the $(\text{Mn}_4)_2$ dimer is accurately described as follows. Each of the Mn_4 subunits has a $S=9/2$ ground state with an additional zero-field splitting of the easy-axis type. Accordingly, the $S=9/2$ level is split into five $\pm M_S$ Kramers

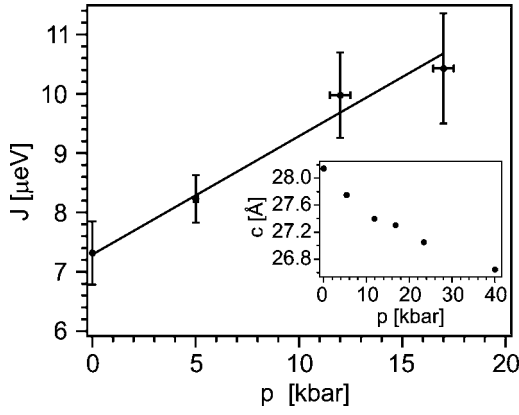


FIG. 4. Dependence of J on pressure p . The solid line represents the least-squares fit Eq. (3). The inset shows the pressure dependence of the unit-cell constant c at room temperature (error bars are smaller than symbol sizes).

doublets, which is well reproduced by the spin Hamiltonian

$$\hat{H}_{ZFS} = D \left(\hat{S}_z^2 - \frac{1}{3} S(S+1) \right) + B_4^0 \hat{O}_4^0(S), \quad (1)$$

where $\hat{O}_4^0(S) = 35\hat{S}_z^4 - 30S(S+1)\hat{S}_z^2 + 25\hat{S}_z^2 + 6S(S+1)$, and the z axis coincides with the threefold symmetry axis (or the c unit-cell axis). In $(\text{Mn}_4)_2$, two identical Mn_4 units are fused together, leading to the following effective spin Hamiltonian for the dimer:

$$\hat{H} = \hat{H}_{ZFS,A} + \hat{H}_{ZFS,B} + J\hat{S}_A \cdot \hat{S}_B. \quad (2)$$

Here, $\hat{H}_{ZFS,A}$ and $\hat{H}_{ZFS,B}$ are centered on the two Mn_4 subunits A and B and have the form of Eq. (1), and $J > 0$ describes the isotropic AFM exchange interaction between the two units. The effect of J is to split the Mn_4 Kramers doublets into two or three components. For instance, the lowest-lying Mn_4 doublet $|M_S = \pm 9/2\rangle$ splits into the two dimer doublets $|M_{S_A} = 9/2, M_{S_B} = -9/2\rangle_{sla}$ and $|M_{S_A} = 9/2, M_{S_B} = 9/2\rangle_{sla}$ as indicated in Fig. 3 (for a detailed classification of the levels, see Ref. 17).

From Hamiltonian (2) INS spectra were calculated as described in Ref. 17. The result of least-squares fits to the data, where the parameters J , D , and B_4^0 (and the linewidth) were chosen as variables, are shown as solid lines in Fig. 2. The agreement between experimental and theoretical curves is excellent. Thanks to the many peaks in the data, the fit parameters could be accurately determined. Within the error bars, a negligibly small pressure dependence of D and B_4^0 was detected: Fitting of the results to a linear dependence yields $D(p) = -62.2(2) \mu\text{eV} - 0.037(32) \mu\text{eV}/\text{kbar} \times p$ and $B_4^0(p) = -7.1(3) \times 10^{-3} \mu\text{eV} + 22(56) \times 10^{-6} \mu\text{eV}/\text{kbar} \times p$. The coupling constant J on the other hand is affected strongly, as shown in Fig. 4. The best-fit line is

$$J(p) = 7.3(4) \mu\text{eV} + 0.20(5) \mu\text{eV}/\text{kbar} \times p. \quad (3)$$

The pressure dependence of the unit-cell parameter c is shown in the inset of Fig. 4. It monotonically decreases from 28.168(1) \AA at 0 kbar to 26.5727(9) \AA at 40 kbar in a qua-

silinear fashion. The cell parameter a and the volume V exhibit pressure dependencies similar to c , with a decrease of a from 16.2991(3) to 15.143(1) \AA and of V from 6480.6(1) \AA^3 to 5276.8(4) \AA^3 in the pressure range 0–40 kbar.

The trigonal symmetry axis of the molecular dimers is collinear with the hexagonal axis of the unit cell, and the decrease of c with pressure directly relates to a decrease of the separation between the Mn_4 subunits within the dimer. At 40 kbar c is decreased by a moderate 6%. Furthermore, the pressure dependence of the volume V shows a quasilinear decrease, showing that the pressure range where repulsive forces between the dimers become significant has not yet been reached. Finally, the bulk modulus B and its pressure derivative were obtained by fitting a universal equation of state.¹⁸ The resulting small bulk modulus of $B = 11$ GPa is consistent with a weak intermolecular bonding. It is hence concluded that the compression under pressure is achieved mostly through reduction in intermolecular space.

The insignificant pressure dependence of D in $(\text{Mn}_4)_2$ is in clear contrast to the observed 4% decrease of D in the SMM Mn_4Br , which is very similar to the Mn_4 subunits in $(\text{Mn}_4)_2$, except that the apical Cl ion is replaced by a Br ion.¹⁹ However, this can be understood by the fact that Mn-Cl bonds are stronger and less compressible than Mn-Br bonds. Thus the Mn_4 subunits of $(\text{Mn}_4)_2$ are less distorted under pressure than the Mn_4Br cluster, which is consistent with the conclusions of the previous paragraph.

In contrast, the J value exhibits a large increase from 7.3(4) to 10.4(9) μeV in the pressure range 0–17 kbar, i.e., an increase of 42%. Interestingly, this change is of the order of what can be achieved by a chemical modification, e.g., a solvent exchange: For the cluster studied here, but with the MeCN solvent molecules replaced by n -hexane molecules, the J value was found to be 10.3(9) μeV , or 43% larger, while the Cl-Cl distance was decreased by 0.13 \AA or 3.4%, respectively.⁴ We conclude that in $(\text{Mn}_4)_2$ the Cl-Cl distance between the two Mn_4 units decreases by about the same amount of ca. 3.4% upon application of 17 kbar. This is further supported by our x-ray experiment, which shows that at 17 kbar the c axis is reduced by 2.6%. This represents a lower limit for the compression of the Cl-Cl distance, assuming a homogeneous compression along c . Considering the stiffness of the Mn_4 subunits derived above, the compression of Cl-Cl will be bigger than 2.6%, and a value of 3.4% or 0.13 \AA at 17 kbar appears very reasonable.

The functional dependence of J on the Cl-Cl distance d can be expressed as $J(d) = J_0 \exp[-k(d-d_0)]$. k is a measure of how fast the overlap of the neighboring wave functions decreases with increasing distance. With J_0 and d_0 the values at 0 kbar, one obtains $k = -2.7(7) \text{\AA}^{-1}$. Recently, the weak exchange between the subunits in the $(\text{Mn}_4)_2$ dimer was studied theoretically by means of density functional theory (DFT) calculations.²⁰ The absolute value of J was calculated about a factor of 2 too large, and for the dependence on the Cl-Cl distance a slope of $k = -2 \text{\AA}^{-1}$ was inferred. The latter value should be reliable as DFT should capture trends better than absolute values. The experiment and the DFT calculation thus show a nice agreement. For comparison, for the distance

dependence of J in iron(III) dimers and trimers values of $k = -6$ and -8 \AA^{-1} were found, respectively.^{21,22} This underpins the soft character of the exchange bridge in the $(\text{Mn}_4)_2$ dimer.

Our results suggest an interesting effect of applied pressure on the magnetic hysteresis curve. Starting from negative magnetic fields, $(\text{Mn}_4)_2$ at ambient pressure undergoes tunneling transitions at fields of ca. -0.35 T (tunneling from $|9/2, 9/2\rangle$ to $|9/2, -9/2\rangle$), at ca. 0.2 T (tunneling from $|9/2, 9/2\rangle$ to $|7/2, -9/2\rangle$), and further transitions at higher fields.¹³ Thus, because of the effect of the interdimer coupling J no tunneling transition at zero field is observed, in remarkable contrast to the behavior in standard SMMs. However, with increasing J the second tunneling transition $|9/2, 9/2\rangle \rightarrow |9/2, -9/2\rangle$ will move to lower and eventually to negative magnetic fields. This can be inferred from Fig. 3. In order to satisfy the tunneling condition of equal energy of both states, the zero-field gap between the states $|9/2, 9/2\rangle$ and $|9/2, -9/2\rangle$ has to be overcome by a magnetic field. These two levels, however, approach each other with increasing J and eventually cross at a value of $J_c = 14.5 \mu\text{eV}$. At this point, the system will exhibit a tunneling transition at zero field analogous to that of standard SMMs. Extrapolating our determined $J(p)$ dependence, this point is estimated to be reached at ca. 36 kbar , which is well within the bounds of possibility in magnetization measurements. Thus, it is predicted that as function of pressure the magnetic hysteresis curve should show strong changes, and that the $(\text{Mn}_4)_2$ dimer system may be tuned into a condition where it exhibits a magnetic hysteresis curve with a step at zero field, more similar to that of conventional SMMs.

In conclusion, we have studied the response of the

dimeric SMM $(\text{Mn}_4)_2$ to hydrostatic pressure, as reflected in changes of INS and powder x-ray diffraction spectra. The magnetic parameters of the Mn_4 subunits were found to be pressure independent up to 17 kbar , in contrast to findings where changes on the order of 4% were observed,^{17,23} but in agreement with the particular chemical situation in this molecule. On the other hand, the interdimer exchange parameter J displayed a pronounced increase by 42% between ambient pressure and 17 kbar . The dependence of J on the Cl-Cl distance between the Mn_4 subunits was estimated and found to be in nice agreement with predictions of DFT calculations, which indicates that DFT calculations are an appropriate tool to study weak long-distance exchange interactions. From our results we predict that within experimentally reasonable pressures the magnetic properties of $(\text{Mn}_4)_2$ will be drastically affected. At a pressure of about 36 kbar the system should exhibit a magnetic hysteresis curve more similar to that of a conventional SMM. This tuning possibility could be interesting for potential applications.

This work demonstrates that the combination of INS and pressure is an excellent tool to study intermolecular magnetic interactions. First, pronounced changes in the magnetic behavior can be induced, which may be as large as those achieved by chemical variations. Second, compared to the application of pressure by chemical means, hydrostatic pressure can be adjusted continuously which allows for many measurement points.

We thank A. J. Church and C. M. Goodway from the ISIS sample environment group for help. Financial support by EC-RTN-QUEMOLNA, Contract No. MRTN-CT-2003-504880, and the Swiss National Science Foundation (NFP 47) is acknowledged.

-
- ¹G. Christou, D. Gatteschi, D. N. Hendrickson, and R. Sessoli, *MRS Bull.* **25**, 66 (2000).
- ²D. Gatteschi and R. Sessoli, *Angew. Chem., Int. Ed.* **42**, 268 (2003).
- ³W. Wernsdorfer and R. Sessoli, *Science* **284**, 133 (1999).
- ⁴S. Hill, R. S. Edwards, N. Aliaga-Alcalde, and G. Christou, *Science* **302**, 1015 (2003).
- ⁵E. del Barco, A. D. Kent, E. C. Yang, and D. N. Hendrickson, *Phys. Rev. Lett.* **93**, 157202 (2004).
- ⁶O. Waldmann, C. Dobe, H. Mutka, A. Furrer, and H. U. Güdel, *Phys. Rev. Lett.* **95**, 057202 (2005).
- ⁷R. Sessoli, D. Gatteschi, A. Caneschi, and M. A. Novak, *Nature (London)* **365**, 141 (1993).
- ⁸J. R. Friedman, M. P. Sarachik, J. Tejada, and R. Ziolo, *Phys. Rev. Lett.* **76**, 3830 (1996).
- ⁹L. Thomas, F. Lioni, R. Ballou, D. Gatteschi, R. Sessoli, and B. Barbara, *Nature (London)* **383**, 145 (1996).
- ¹⁰Y. Hosokoshi, Y. Nakazawa, K. Inoue, K. Takizawa, H. Nakano, M. Takahashi, and T. Goto, *Phys. Rev. B* **60**, 12924 (1999).
- ¹¹T. Nikuni, M. Oshikawa, A. Oosawa, and H. Tanaka, *Phys. Rev. Lett.* **84**, 5868 (2000).
- ¹²C. Rüegg, N. Cavadini, A. Furrer, H. U. Güdel, K. Krämer, H. Mutka, A. Wildes, K. Habicht, and P. Vorderwisch, *Nature (London)* **423**, 62 (2003).
- ¹³W. Wernsdorfer, N. Allaga-Alcalde, D. N. Hendrickson, and G. Christou, *Nature (London)* **416**, 406 (2002).
- ¹⁴D. N. Hendrickson, G. Christou, E. A. Schmitt, E. Libby, J. S. Bashkin, S. Y. Wang, H. L. Tsai, J. B. Vincent, P. D. W. Boyd, J. C. Huffman, K. Folting, Q. Y. Li, and W. E. Streib, *J. Am. Chem. Soc.* **114**, 2455 (1992).
- ¹⁵A. Hammersley (private communication).
- ¹⁶J. Rodriguez-Carvajal (private communication).
- ¹⁷A. Sieber, D. Foguet-Albiol, O. Waldmann, S. T. Ochsenbein, R. Bircher, G. Christou, F. Fernandez-Alonso, H. Mutka, and H. U. Güdel, *Inorg. Chem.* **44**, 6771 (2005).
- ¹⁸P. Vinet, J. R. Smith, J. Ferrante, and J. H. Rose, *Phys. Rev. B* **35**, 1945 (1987).
- ¹⁹A. Sieber, G. Chaboussant, R. Bircher, C. Boskovic, H. U. Güdel, G. Christou, and H. Mutka, *Phys. Rev. B* **70**, 172413 (2004).
- ²⁰K. Park, M. R. Pederson, S. L. Richardson, N. Aliaga-Alcalde, and G. Christou, *Phys. Rev. B* **68**, 020405(R) (2003).
- ²¹S. M. Gorun and S. J. Lippard, *Inorg. Chem.* **30**, 1625 (1991).
- ²²H. Weihe and H. U. Güdel, *J. Am. Chem. Soc.* **119**, 6539 (1997).
- ²³A. Sieber, R. Bircher, O. Waldmann, G. Carver, G. Chaboussant, H. Mutka, and H. U. Güdel, *Angew. Chem., Int. Ed.* **44**, 4239 (2005).